PHYSICAL REVIEW C VOLUME 26, NUMBER 4 OCTOBER 1982

Configuration space Faddeev continuum calculations. I. *n-d* scattering length

G. L. Payne
Department of Physics and Astronomy, University of Iowa, Iowa City, Iowa 52242

J. L. Friar and B. F. Gibson
Theoretical Division, Los Alamos National Laboratory, Los Alamos, New Mexico 87545
(Received 1 June 1982)

Formulation of the zero-energy Faddeev-type scattering equations in configuration space is discussed. Numerical solutions are obtained using spline techniques. Scattering lengths are calculated for the *s*-wave *NN* interaction models of Malfliet and Tjon; comparison with previously published results and Kohn variational estimates are made. Faddeev amplitudes and Schrödinger wave functions are plotted. Significant features of the configuration space solutions are identified.

[NUCLEAR REACTIONS ^{2}H$(n,n)^2$H, $E=0$ MeV; *n-d* scattering lengths; configuration space Faddeev calculation.]

I. INTRODUCTION

Total binding energies and nucleon separation energies are two of the most precisely determined quantities known in nuclear physics. But these, and other less precisely measured bound-state properties such as the root mean square (rms) radius, provide a rather restricted set of data with which to test our understanding of the complexities of the basic nuclear force. It is the scattering problem, where cross sections as a function of energy, angular distributions, and polarization phenomena can be measured, which offers us the opportunity to explore the accuracy of our knowledge of the nucleon-nucleon strong interaction. The natural beginnings of such a program lie in the "simple" three-nucleon continuum problem. But a proper theoretical statement of the quantum mechanical three-body problem eluded our grasp for many years, frustrating researchers and generating misleading approximations as well as incorrect interpretation of data.

The motivation for Faddeev's revolutionary work[1] on the *t*-matrix approach to the three-body problem was the fact that the boundary conditions in a Lippmann-Schwinger equation formulation of this scattering problem are ill defined. Although the bound-state boundary conditions permit one to work directly with the Schrödinger equation for local potential ^{3}H-^{3}He calculations,[2,3] there are advantages in utilizing the "Faddeev" type formalisms even for trinucleon bound-state studies.[3,4] However, for the continuum three-body local potential problem one must make the Faddeev decomposition (or its equivalent) of the scattering amplitude in order to enforce the proper boundary conditions; the Lippman-Schwinger equation does not yield a unique solution. Part of the purpose in this paper is to remove some of the mystique associated with the term "Faddeev calculation" by the nonexpert. To that end we address the zero-energy *nd* scattering length problem as being the simplest to follow.

We choose to work in configuration space rather than momentum space, because we wish to explore the wave function of three-body continuum states in terms of spatial coordinates. These are the more familiar coordinates for discussing the nucleon-nucleon scattering wave function and for which our intuition is stronger. It is our purpose to provide that same intuitive feeling for "exact" three-body scattering wave functions. Prior to publishing detailed studies and applications of the continuum wave functions we report here on our numerical methods and their convergence properties and compare our scattering length results with those previously published, as well as with bounds obtained from the Kohn variational procedure.[5] We study the *nd* scattering lengths for the (partial-wave) local potential models of Malfliet and Tjon[6] in which the nucleon-nucleon interaction is nonzero only for the *s* wave. We compare spin doublet and quartet scattering lengths with the momentum space calculations of Tjon,[7] the unitary pole approximation cal-

culations of Harms and Newton,[8] and the configuration space calculations of Benayoun, Gignoux, and Chauvin.[9] The most informative comparisons are with our Kohn variational results where identical potential parameters are used for each calculation.

In Sec. II of this paper we review the three-body scattering equations for the specific case of three pairwise interacting bosons in an attempt to make the problem transparent. (The spin-isospin coupled equations for the fermion problem are summarized in the Appendix.) In Sec. III we discuss the corresponding Kohn variational procedure. In Sec. IV we outline our numerical methods; in particular we discuss our application of spline functions in the context of orthogonal collocation. We provide a detailed account of our numerical results in Sec. V. In Sec. VI we present graphical representations of wave functions and their components. We summarize our conclusions in Sec. VII.

II. THREE-BODY EQUATIONS IN CONFIGURATION SPACE

While the Faddeev equations for three pairwise interacting bosons have the same form for bound state and scattering problems, the boundary conditions for these two problems are considerably different.[10–14] The bound-state wave function asymptotically approaches zero for large values of any two-particle separation. This boundary condition is straightforward to implement.[3,11] Although the bound-state problem is numerically difficult there is little question about the validity of the boundary conditions. For the continuum problem the wave function is nonzero in the asymptotic region,[10,14] and the solution of the Faddeev equations is consequently more sensitive to proper implementation of the boundary conditions. In this section we first review the Faddeev equations for three bosons, and then we discuss the appropriate zero-energy boundary conditions. The corresponding equations for particles with spin are summarized in the Appendix.

Following Ref. 3 we decompose the solution of the Schrödinger equation, Ψ, in terms of the nonphysical auxilliary function, ψ, which is the Faddeev amplitude:

$$\Psi=\psi(\vec{x}_1,\vec{y}_1)+\psi(\vec{x}_2,\vec{y}_2)+\psi(\vec{x}_3,\vec{y}_3) \equiv\psi_1+\psi_2+\psi_3 , \tag{1}$$

where we have used the Jacobi coordinates

$$\vec{x}_i=\vec{r}_j-\vec{r}_k$$

and

$$\vec{y}_i=\tfrac{1}{2}(\vec{r}_j+\vec{r}_k)-\vec{r}_i \tag{2}$$

for the three particles having coordinates $\vec{r}_1$, $\vec{r}_2$, and $\vec{r}_3$. The Schrödinger equation

$$\left[T+\sum_i V(x_i)-E\right]\Psi=0$$

can be decomposed into three coupled Faddeev equations

$$[T+V(x_i)-E]\psi_i=-V(x_i)[\psi_j+\psi_k] , \tag{3}$$

where T is the kinetic energy operator and $V(x_i)$ is the two-body potential representing the interaction between particles j and k. For three identical particles the three Faddeev amplitudes have identical functional forms, and it is only necessary to solve one of the coupled equations.

For s-wave interactions only the $l=0$ partial wave of ψ_1 is nonzero, where l is the relative orbital angular momentum of particles 2 and 3. Using the reduced wave function $\phi(x_1,y_1)$ defined by

$$\phi(x_1,y_1)=x_1y_1\psi(x_1,y_1) , \tag{4}$$

the Faddeev equation can be rewritten in the form

$$\left[\frac{\partial^2}{\partial x_1^{\,2}}+\frac{3}{4}\frac{\partial^2}{\partial y_1^{\,2}}-U(x_1)+K^2\right]\phi(x_1,y_1) = U(x_1)\int_{-1}^{1}d\mu\frac{x_1y_1}{x_2y_2}\phi(x_2,y_2) , \tag{5}$$

where $K^2=mE/\hbar^2$, $U(x_1)=mV(x_1)/\hbar^2$, and m is the nucleon mass. Using Eq. (2) one can easily verify that

$$x_2=\tfrac{1}{2}(x_1^{\,2}-4x_1y_1\mu+4y_1^{\,2})^{1/2} , \tag{6a}$$

$$x_3=x_2(-\mu) , \tag{6b}$$

$$y_2=\tfrac{1}{2}(\tfrac{9}{4}x_1^{\,2}+3x_1y_1\mu+y_1^{\,2})^{1/2} , \tag{6c}$$

$$y_3=y_2(-\mu) , \tag{6d}$$

where μ is the cosine of the angle between x_1 and y_1.

Since Eq. (5) is an elliptic partial differential equation, the boundary conditions must be specified on a closed surface. For the reduced wave function the boundary conditions along the x_1 axis and the y_1 axis are the same as for the bound state problem,

$$\phi(0,y_1)=\phi(x_1,0)=0 . \tag{7}$$

It is the boundary condition for the asymptotic region ($x_1\rightarrow\infty$ or $y_1\rightarrow\infty$) which complicates the

continuum problem. For the scattering of one particle from a bound cluster of the remaining two particles above the threshold energy for breakup of the bound two-body cluster, the boundary conditions are difficult to write in closed form, and one must use approximations to the exact boundary conditions.[13] For energies below the threshold for breakup the problem is considerably simpler, and such is the case which we consider; we show that one can define boundary conditions which are exact in the same sense as the bound state boundary condition. For the scattering length problem the incident particle has zero energy and the total energy of the system is just the two-body binding energy

$$E=-E_d=-(\hbar\kappa)^2/m\ .$$

Using Green's function techniques, it can be shown that for this case

$$\phi(x_1,y_1)\underset{y_1\to\infty}{\to}(y_1-a)u_d(x_1)\ , \tag{8}$$

where $u_d(x_1)$ is the two-body bound-state reduced wave function and a is the scattering length. This form is clearly consistent with the two-body nature of the process and is obtained from the integral equation for $\phi(x_1,y_1)$:

$$\phi(x_1,y_1)=y_1u_d(x_1)-\tfrac{4}{3}\int_0^\infty dy_1' y_< \int_0^\infty dx_1' u_d(x_1)u_d(x_1') \times U(x_1')\int_{-1}^{1}d\mu'\frac{x_1'y_1'}{x_2'y_2'}\phi(x_2',y_2') +\phi_{\rm br}(x_1,y_1)\ . \tag{9}$$

Here $y_<$ is the lesser of y_1 and y_1', and $\phi_{\rm br}$ is the virtual three-body breakup part of the wave function which must vanish for large separations of the interacting particles. For x_1 greater than the range of $U(x_1)$ the virtual breakup term has the form[10]

$$\phi_{\rm br}(x_1,y_1)=A(\theta)e^{-\kappa\rho}/\rho^{1/2}\ , \tag{10}$$

where we have introduced the variables ρ and θ defined by

$$x_1=\rho\cos\theta\ ,\qquad y_1=\frac{\sqrt{3}}{2}\rho\sin\theta\ . \tag{11}$$

Since $\phi_{\rm br}$ is exponentially decreasing for large values of ρ, we can assume that it is zero in the asymptotic region. In this sense the boundary conditions are the same as for the bound state problem, but now we have the additional condition given in Eq. (8). The implementation of this additional boundary condition is discussed in Sec. IV. For large values of ρ these boundary conditions are exact for all values of θ; thus, if the matching radius is large enough no errors will be introduced into the wave function by the boundary conditions. From Eq. (9) one obtains the integral expression for the scattering length:

$$a=\tfrac{4}{3}\int_0^\infty dy_1y_1\int_0^\infty dx_1u_d(x_1)U(x_1) \times\int_{-1}^{1}d\mu\frac{x_1y_1}{x_2y_2}\phi(x_2,y_2)\ . \tag{12}$$

Thus, given the numerical solution to Eq. (5), one can extract the scattering length either by looking at the asymptotic form of $\phi(x_1,y_1)$ or by evaluating the integral in Eq. (12). For our calculations we have used both techniques, and we find that the two values are consistent with one another. A third method for determining the scattering length involves use of the Kohn variational principle. This will be discussed in the next section.

III. THE KOHN VARIATIONAL PRINCIPLE

The Kohn variational principle has been derived for the three particle scattering problem by several authors.[5] In this section we briefly outline the derivation of the scattering length result using the notation of the previous section. The Schrödinger equation for three particles with energy $-E_d$ can be written in the form

$$(-\Delta+U+\kappa^2)\Psi=0\ , \tag{13}$$

where Δ is $-m/\hbar^2$ times the kinetic energy operator and $U=U(x_1)+U(x_2)+U(x_3)$ is $m/\hbar^2$ times the sum of the pairwise interactions. First, consider the matrix element

$$I=\langle\Psi\,|\,(-\Delta+U+\kappa^2)\,|\,\Psi\rangle\ . \tag{14}$$

By varying Ψ we obtain

$$\begin{aligned}\delta I&=\langle\delta\Psi\,|\,(-\Delta+U+\kappa^2)\,|\,\Psi\rangle\\&\quad+\langle\Psi\,|\,(-\Delta+U+\kappa^2)\,|\,\delta\Psi\rangle\\&=\langle\Psi\,|\,(-\Delta+U+\kappa^2)\,|\,\delta\Psi\rangle\ ,\end{aligned} \tag{15}$$

where we have used the fact that Ψ is the exact solution of the Schrödinger equation. Integrating by parts, noting that everything but boundary terms vanish, and using the boundary conditions

$$\begin{aligned}&\psi_i\underset{x_i\to\infty}{\to}0\ ,\\&\delta\psi_i\underset{x_i\to\infty}{\to}0\ ,\end{aligned} \tag{16}$$

and

$$\begin{aligned}&\psi_i\underset{y_i\to\infty}{\to}\frac{(y_i-a)u_d(x_i)}{x_iy_i}\ ,\\&\delta\psi_i\underset{y_i\to\infty}{\to}\frac{-\delta a u_d(x_i)}{x_iy_i}\ ,\end{aligned} \tag{17}$$

one can show that

$$\delta I=-\tfrac{9}{4}\delta a\ . \tag{18}$$

Therefore, we have

$$\delta[I+\tfrac{9}{4}a]=0\ . \tag{19}$$

Now, let $\tilde{I}$ be the matrix element evaluated using the approximate wave function $\tilde{\Psi}$ with a scattering length $\tilde{a}$, and let I be the matrix element evaluated using the true wave function having scattering length a. Then we have the following second-order relationship:

$$\delta[I+\tfrac{9}{4}a]\simeq(I-\tilde{I})+\tfrac{9}{4}(a-\tilde{a})+0(\delta\Psi^2)\ . \tag{20}$$

Thus, using the fact that Eqs. (13) and (14) imply $I=0$, we obtain

$$a\simeq\tilde{a}+\tfrac{4}{9}\tilde{I}\ . \tag{21}$$

This expression provides a variational estimate of the scattering length, which is accurate to second order. We have assumed in this derivation that the deuteron wave function is accurately known for a given potential and need not be varied. For systems where there is no bound state, methods similar to those used in the bound-state problem lead to the bound $\tilde{I}\geq 0$; thus $a\geq\tilde{a}$ follows from Eq. (21). The quartet (three-fermion) system is an example; the Kohn estimate is an upper bound with respect to the value extracted from the asymptotic part of the wave function. For three-fermion doublet scattering the usefulness of the Kohn estimate as an upper bound depends upon the overlap of the continuum wave function with the bound-state wave functions of the same Hamiltonian, just as one finds in making variational estimates of excited state energies of a bound system.[15] The overlap is zero, of course, for exact wave functions but not for (approximate) numerically calculated ones.

IV. NUMERICAL METHODS

In order to numerically evaluate the solution of the Faddeev equations, we make the usual change of variables to the ρ-θ coordinates defined in Eq. (11). Following Ref. 3 we express the solution of the differential equation in terms of bicubic splines on a rectangular grid in these ρ-θ coordinates. From the asymptotic form of the reduced wave function given in Eq. (8) one can see that for large values of ρ and values of θ near $\pi/2$ the solution will have the form

$$(\tfrac{1}{2}\sqrt{3}\rho\sin\theta-a)u_d(\rho\cos\theta)\ .$$

This function varies rapidly with θ because of the structure of the two-body bound-state wave function. This rapid variation with θ for large values of ρ requires a rather fine θ grid for θ near $\pi/2$. The numerical calculation is greatly facilitated if this variation due to the two-body bound state wave function is removed from the equations. Our preliminary approach to the problem was similar to that of Ref. 9, but it was found to be not sufficiently stable. Therefore, we define the smoother function $F(x_1,y_1)$ by

$$\phi(x_1,y_1)=[y_1-F(x_1,y_1)]u_d(x_1)\ . \tag{22}$$

The differential equation for $F(x_1,y_1)$ is then given by

$$u_d(x_1)\left[\frac{\partial^2 F}{\partial x_1^{\,2}}+\frac{3}{4}\frac{\partial^2 F}{\partial y_1^{\,2}}\right]+2u_d'(x_1)\frac{\partial F}{\partial x_1}-U(x_1)\int_{-1}^{1}d\mu\frac{x_1y_1}{x_2y_2}F(x_2,y_2)u_d(x_2)$$
$$=-U(x_1)\int_{-1}^{1}d\mu\frac{x_1y_1}{x_2y_2}[y_2u_d(x_2)]\,, \quad (23)$$

where $u_d'(x_1)$ is the first derivative of $u_d(x_1)$. Since $u_d(0)=0$, the function F has a nonzero value at $x_1=0$. The appropriate boundary condition can be obtained from Eq. (23) evaluated at $x_1=0$. Rewriting this equation in terms of the ρ-θ variables we obtain

$$u_d(\rho\cos\theta)\left[\frac{\partial^2 F}{\partial\rho^2}+\frac{1}{\rho}\frac{\partial F}{\partial\rho}+\frac{1}{\rho^2}\frac{\partial^2 F}{\partial\theta^2}\right]+2u_d'(\rho\cos\theta)\left[\cos\theta\frac{\partial F}{\partial\rho}-\frac{\sin\theta}{\rho}\frac{\partial F}{\partial\theta}\right]$$
$$-U(\rho\cos\theta)\frac{4}{\sqrt{3}}\int_{\theta^-}^{\theta^+}d\theta' F(\rho,\theta')u_d(\rho\cos\theta')=-2U(\rho\cos\theta)\int_{\theta^-}^{\theta^+}d\theta'\rho\sin\theta' u_d(\rho\cos\theta')\,, \quad (24)$$

where the limits of integration θ^+ and θ^- are defined in Ref. 3.

For large values of y_1 the function $F(x_1,y_1)$ approaches a constant value, which is the scattering length a. Therefore, for large values of ρ we impose the boundary condition along $\rho=\rho_{\max}$

$$\frac{\partial F}{\partial\rho}=0\,, \quad (25)$$

Using this boundary condition together with

$$F(\rho,0)=0\,, \quad (26)$$

and the boundary condition for $F(\rho,\pi/2)$ which follows from Eq. (23), we can obtain a unique solution to the elliptic integrodifferential equation. The boundary condition defined in Eq. (25) is clearly correct for large values of y_1, but one may question its validity for large values of x_1 and small values of y_1. To check the accuracy of the solution obtained using the boundary condition in Eq. (25), we have used Eq. (9) to determine an improved boundary condition as follows. Using the integral expression in Eq. (9) one finds for large values of ρ (where $\phi_{\rm br}$ can be neglected) that

$$\frac{\partial F}{\partial\rho}=\cos\theta\frac{\partial F}{\partial x}+\frac{\sqrt{3}}{2}\sin\theta\frac{\partial F}{\partial y}$$
$$=\frac{2}{\sqrt{3}}\sin\theta\int_{y_1}^{\infty}dy_1'\int_0^{\infty}dx_1'u_d(x_1')U(x_1')\int_{-1}^{1}d\mu\frac{x_1'y_1'}{x_2'y_2'}[y_2'-F(x_1',y_2')]u_d(x_2')\,. \quad (27)$$

For large values of y_1 this reduces to Eq. (25). Using the solution F obtained from Eq. (24) with the boundary condition defined by Eq. (25), we obtain an improved boundary condition by iteration using Eq. (27). This iterative process can be repeated until a consistent solution F is obtained; i.e., subsequent iteration produces no change in a. In practice it was found that iterating the boundary condition produced no significant improvement in the wave function. The errors produced by the approximate boundary condition defined in Eq. (25) tend to "heal" quickly because the wave function is exponentially decaying in that region.

For the actual numerical calculation we express the function $F(\rho,\theta)$ as a bicubic spline on a rectangular grid in the ρ-θ coordinates.[3] We take advantage of the fact that the knots for the splines do not have to be equally spaced. We scale in the θ variable such that $(\theta_{n+1}-\theta_n)=(\theta_n-\theta_{n-1})S_\theta$, where S_θ is the scale factor. In the ρ variable we take advantage of the slow variation of $F(\rho,\theta)$ for larger values of ρ by scaling as for θ inside a radius $\rho_{\rm br}$ and using a uniform distribution of splines between $\rho_{\rm br}$ and $\rho_{\max}$. A discussion of the treatment of the analogous problem for particles with spin can be found in the Appendix.

V. NUMERICAL RESULTS

We study in detail the stability, accuracy, and convergence of our configuration space solution of

TABLE I. Potential parameters for the Malfliet-Tjon models.

Model	V_A (MeV fm)	μ_A (fm^{-1})	V_R (MeV fm)	μ_R (fm^{-1})	B_2 (MeV)
I	513.968	1.550	1438.720	3.110	
II	52.490	0.809	0		
III	626.885	1.550	1438.720	3.110	2.23
IV	65.120	0.633	0		2.23
V	570.316	1.550	1438.4812	3.110	0.35

the zero-energy scattering length problem utilizing the s-wave potential model forms of Malfliet and Tjon.[6] These partial-wave-local two-body potentials are sums of Yukawa forms exhibiting a long-range attraction and (in most cases) a short-range repulsion

$$V(r)=(V_R e^{-\mu_R r}-V_A e^{-\mu_A r})/r \ . \tag{28}$$

We emphasize that these potentials act only in the $l=0$ two-body partial waves; that is, they may be considered to have s-wave projection operators associated with them. Thus, the zero-energy "nd" scattering wave functions have only $L=0$ partial waves. Correspondingly, the continuum wave functions for the fermion problem are specified by the intrinsic spins of the states ($S=\frac{1}{2}$ doublet and $S=\frac{3}{2}$ quartet), since $J=S$. For the model problems in which we use an average spin-singlet, spin-triplet potential the fermion doublet solution and the boson solution are identical.

The parameters defining the specific potential models studied are given in Table I. They differ slightly from those which one might infer from Ref. 6, as has been noted previously.[3,15] Our parameter values were chosen to reproduce the physical two-body binding energies quoted in Ref. 6; we have used $\hbar^2/m=41.47$ MeV fm^2 throughout this work.

Because the MT III (spin-triplet) potential provides the most realistic description of the deuteron properties, we consider this model in greatest detail. It should provide the most realistic test of our accuracy and convergence in a simple one-channel calculation. To this end we list in Table II the mesh parameter values for a selection of the test cases which we explored. The corresponding boson (or doublet) and quartet scattering lengths are compiled

TABLE II. Mesh parameters used in the study of the accuracy and convergence of the scattering length calculations for the MT III potential model.

Case No.	N_I	N_E	$\rho_{\rm br}$	S_ρ	$\rho_{\rm max}$	N_θ	S_θ
1	20	10	10.0	1.3	70.0	20	1.3
2	16	10	10.0	1.3	70.0	20	1.3
3	16	8	10.0	1.3	58.0	20	1.3
4	16	6	10.0	1.3	46.0	20	1.3
5	16	4	10.0	1.3	34.0	20	1.3
6	16	3	10.0	1.3	28.0	20	1.3
7	12	8	10.0	1.3	70.0	20	1.3
8	12	8	8.0	1.3	70.0	20	1.3
9	12	8	15.0	1.3	70.0	20	1.3
10	12	10	10.0	1.3	70.0	20	1.3
11	10	10	10.0	1.3	70.0	20	1.3
12	12	12	10.0	1.3	70.0	20	1.3
13	12	8	10.0	1.3	58.0	20	1.3
14	16	10	10.0	1.2	70.0	20	1.3
15	16	10	10.0	1.4	70.0	20	1.3
16	16	10	10.0	1.3	70.0	18	1.3
17	16	10	10.0	1.3	70.0	16	1.3
18	16	10	10.0	1.3	70.0	14	1.3
19	16	10	10.0	1.3	70.0	20	1.25
20	16	10	10.0	1.3	70.0	20	1.50

TABLE III. Doublet (boson) and quartet scattering lengths a_2 and a_4 along with their Kohn variational estimates for the MT III potential model of Table I.

Case No.	a_2	a_2^K	a_4	a_4^K
1	26.033	26.033	6.4412	6.4416
2	26.030	26.033	6.4411	6.4416
3	26.028	26.033	6.4381	6.4392
4	26.026	26.031	6.4189	6.4197
5	25.999	26.003	6.2843	6.2847
6	26.022	26.024	6.0500	6.2506
7	26.037	26.037	6.4413	6.4416
8	26.001	26.038	6.4400	6.4416
9	25.989	26.035	6.4413	6.4416
10	26.014	26.035	6.4411	6.4416
11	25.987	26.036	6.4410	6.4416
12	26.000	26.034	6.4405	6.4416
13	26.012	26.035	6.4381	6.4392
14	26.040	26.033	6.4412	6.4416
15	26.012	26.035	6.4411	6.4416
16	26.037	26.037	6.4340	6.4416
17	26.104	26.034	6.3839	6.4417
18	26.721	25.971	6.0587	6.4483
19	26.045	26.034	6.4402	6.4418
20	26.048	26.036	6.4414	6.4416

in Table III. We provide both the value extracted from the asymptotic wave function and the Kohn variational estimate (superscript K) based upon that wave function. The boson or doublet scattering length a_2 is some four times larger than the quartet scattering length a_4. It is also the scattering length of the spin-isospin channel in which the two-body potentials support a bound state. Therefore, we direct our comments concerning the accuracy and convergence primarily to the a_2 results.

As was true in our study of the bound state, the sensitivity of the solution to the ρ-grid parameters proved to be the more complex. Convergence with respect to the cutoff radius $\rho_{\max}$ is obtained by about 45 fm. (A somewhat larger value is required for a_4.) Solutions with 0.1% accuracy can be obtained with smaller values of $\rho_{\max}$, but the oscillation of a_2 and a_2^K imply that the intrinsic accuracy is less than the raw numbers might indicate. (In particular, the apparent 0.01 uncertainty in the a_2 values for $\rho_{\max}=28$ fm is misleading.) A value for the parameter $\rho_{\rm br}$ lying somewhere between 10.0 and 12.0 fm appears to be optimal; again 0.1% accuracy can be achieved with a wider range of values (e.g., 8.0 to 15.0 fm). We find that at least 10 to 12 points inside $\rho_{\rm br}$ are required to provide a reasonable description of the interior part of the solution. A scale factor S_ρ lying between 1.2 and 1.4 provides reasonable results, with $S_\rho=1.3$ providing the best spacing for the nonuniform distribution of ρ points in the interior region. As was the case for the bound state, we anticipate that more points will be required in the interior region near the origin when using more repulsive potentials such as the Reid-soft-core model.[16] In the exterior region where the wave function is relatively smooth, a uniform spacing between ρ points of as large as 6–7 fm is feasible. Sensitivity of the solution to the θ grid is similar to that found previously for the bound state problem: More points are required than in the ρ grid; at least 18 θ-grid points were needed to produce an accurate a_2 value. As discussed above, we find it necessary to concentrate the points in the region where the deuteron bound state function is important, even though we have factored that function ϕ_d out of the equation we solve. A scale factor S_θ of between 1.25 and 1.5 gives reasonable results.

Our best estimates of a_2 and a_4 for the MT III potential model are 26.03 ± 0.01 fm and 6.442 ± 0.005 fm, respectively. The agreement between the values extracted from the asymptotic part of the wave function (quoted in Table III) and those obtained from the integral over the entire wave function (26.034 fm for case 1) were normally excellent. Disagreement between the scattering length values obtained from the two methods proved to be

a reliable indicator that neither value would be confirmed by the Kohn variational estimates using that same wave function. (For example, the integral results for case 18 were 28.151 and 6.6055.) We note here that, as is the case for the bound state problem,[15] the Faddeev solution for the scattering length need not lie above the variational bound provided by the Kohn result. Nevertheless, as one would anticipate from a variational procedure that even wave functions which do not provide a good extracted value of the scattering length do yield reasonable Kohn estimates. Our value of the boson scattering length a_2 cannot be compared with results from the literature because none were found. However, quoted values for a_4 are 6.35 fm by Tjon,[7] 6.47 fm by Harms and Newton,[8] and 6.4 fm by Benayoun, Gignoux, and Chauvin.[9] One cannot be certain that the two-body potentials used in each of these calculations were identical, and agreement between our best estimate of a_2 and these values is probably satisfactory. Therefore, comparison of the scattering length values extracted from our wave function and the Kohn variational estimates is probably the more suitable indication of the precision of our solution.

The MT V potential model is not a realistic description of the physics of either the spin-singlet or the spin-triplet nucleon-nucleon interaction, although it is a reasonable average potential for simple, model three-body bound-state calculations. However, its weak two-body binding of 0.35 MeV provides an interesting test of the accuracy of our method when the two-body bound-state wave function has a very large spatial extent. For this model we estimate values of $a_2=34.9\pm0.2$ fm and $a_4=14.1\pm0.5$ fm. As was the case for the MT III calculations, the quartet scattering length proved to be more sensitive to $\rho_{\max}$ than the doublet. We used values of $\rho_{\max}$ as large as 100.0 fm in an effort to obtain an accurate a_4 solution; a_4 was still slowly increasing.

The MT IV model (no repulsion) has been studied previously in the case of the quartet scattering length. Values of 6.45 and 6.47 fm were obtained in Refs. 7 and 8, respectively. Using the potential parameters quoted in Table II, we obtain an estimate of $a_4=6.53\pm0.01$ fm. Again, differences between our value and those previously obtained may be due to the use of slightly different potential parameters.

We now turn to the more interesting problem of estimating the doublet scattering length a_2 when the model admits spin dependence of the two-body forces, producing a coupled-channel set of equations to be solved. (See the Appendix.) Because of the practical limitations imposed by computer memory, the meshes with which we could work had to be reduced from those utilized in the one-channel studies; however, we have seen above that reasonable one-channel solutions can be achieved with fewer than 20 ρ points. Sample results for the MT I-III model are shown in Table IV. Our best estimate, which does not necessarily correspond to any one set of parameters shown in Table IV, is $a_2=0.70\pm0.01$ fm. The Kohn variational results indicate that our scattering length values determined from the asymptotic part of the scattering wave function (a_2) and from the integral over the entire wave function ($a_2^{\int}$) are quite accurate. The uncertainties in our solutions are rather well understood. For comparison we quote the results of Tjon[7] who obtained 0.9 fm, the results of Harms and Newton[8] who obtained 0.92 fm, and the results of Benayoun, Gignoux, and Chauvin[9] who obtained 0.62 fm. Again, we point out that differences may be due in part to the use of slightly different parameters for the MT I-III potentials.

The corresponding calculation for the MT II-IV

TABLE IV. Sample doublet scattering length results for the MT I-III model obtained for typical mesh parameters; a_2^K is the Kohn estimate and $a_2^{\int}$ is the value calculated using the integral over the entire wave function.

N_I	12	12	10	10	10	10	10
N_E	8	8	10	8	10	6	4
$\rho_{\rm br}$	10.0	10.0	10.0	10.0	10.0	10.0	10.0
S_ρ	1.3	1.3	1.3	1.3	1.3	1.3	1.3
$\rho_{\max}$	70.0	70.0	70.0	58.0	58.0	46.0	34.0
N_θ	20	20	20	20	20	20	20
S_θ	1.4	1.3	1.3	1.3	1.3	1.3	1.3
a_2	0.693	0.689	0.695	0.696	0.698	0.704	0.782
a_2^K	0.701	0.701	0.701	0.702	0.702	0.711	0.788
$a_2^{\int}$	0.691	0.686	0.693	0.694	0.695	0.708	0.774

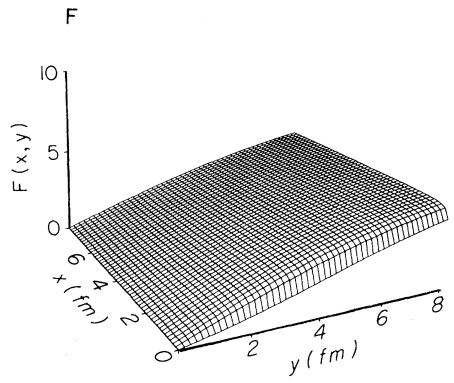

FIG. 1. Faddeev amplitude component F for the MT III potential model quartet solution.

model yields a value of $a_2 = -5.6 \pm 0.1$ fm. This is to be compared with -5.3 fm from Ref. 7 and -1.11 fm from Ref. 8. Clearly, repulsion in the two-body interactions is important in treating doublet scattering, where the Pauli principle is not the dominant factor.

VI. FADDEEV AMPLITUDE AND SCHRÖDINGER WAVE FUNCTION COMPARISONS

An intuitive feeling for the wave function of the continuum system is required if one is to achieve a true understanding of the *nd* scattering problem. A knowledge of the structure of this wave function is also required if one is to ascertain why certain calculational approaches succeed while other procedures flounder in difficulty. For these reasons we present here a brief graphical study of the wave functions generated using the MT I-III potential model. The appropriate wave functions are defined in the Appendix. We depict for the first time in

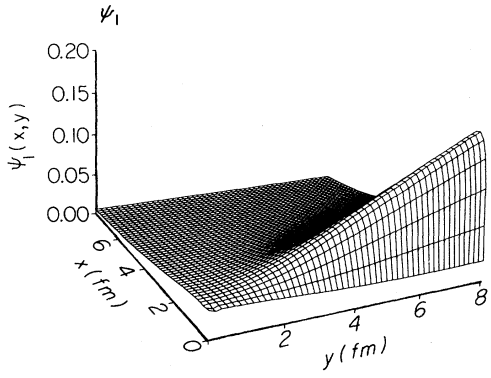

FIG. 2. Faddeev amplitude ψ_1 for the MT III potential model quartet solution.

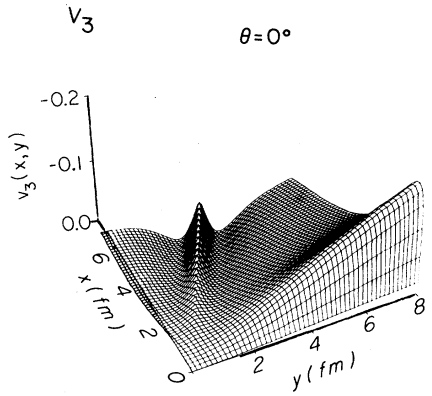

FIG. 3. Quartet Schrödinger wave function component v_3 at fixed angle $\theta = 0°$ for the MT III potential model.

three dimensions the configuration space characteristics of these continuum functions and point out the important features.

For s-wave potentials, which we consider here, the Faddeev amplitudes are functions of only the two variables x_1 and y_1, whereas the full Schrödinger solution depends upon all three variables x_1, y_1, and θ, the angle between $\vec{x}_1$ and $\vec{y}_1$. (We used $\mu = \cos\theta$ as the convenient variable in Sec. II.) The θ dependence of the Schrödinger wave function (Ψ for the quartet or u, v_1, and v_2 components for the doublet) comes from the permuted variables in ψ_2 and ψ_3, as is true for the bound-state problem. Furthermore, although the Faddeev amplitudes $\psi(x_1,y_1)$ generated from the s-wave two-body potentials of our model contain only $l = 0$ relative orbital angular momentum, the total wave function contains all partial waves, just as ψ_2 and ψ_3 do.

The MT I-III potentials exhibit short range repul-

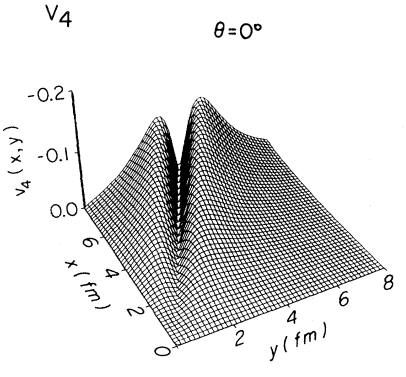

FIG. 4. Quartet Schrödinger wave function component v_4 at fixed angle $\theta = 0°$ for the MT III potential model.

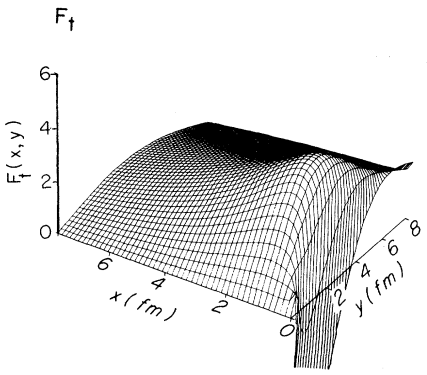

FIG. 5. Faddeev amplitude component F_t for the MT I-III potential model doublet solution.

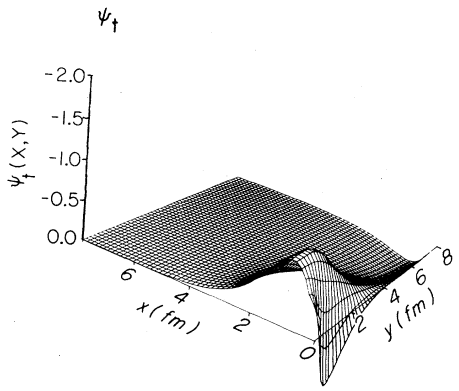

FIG. 7. Faddeev amplitude ψ_t for the MT I-III potential model doublet solution.

sion. Even so, the Pauli principle dominates the quartet scattering length problem to such an extent that the resulting wave function shows few of the interesting characteristics of the doublet scattering problem. We therefore limit our consideration of the zero-energy quartet continuum functions to Figs. 1—4. For convenience we use $x \equiv x_1$ and $y \equiv y_1$ in what follows. We plot as a function of x and y, holding θ fixed.

In Fig. 1 we see $F(x,y)$ as defined in Eq. (22). By removing the $u_d(x)$ dependence from ψ_1, we have reduced the numerical problem to one of generating a considerably smoother function. [Note that $F(x,y) \to a_4$ asymptotically with y; we have not plotted this function out to the asymptotic region.] The simplification can be appreciated by comparing F with the Faddeev amplitude ψ_1 (see Fig. 2) which does contain the deuteron structure. In Figs. 3 and 4 we see the Schrödinger wave function components v_3 and v_4 corresponding to $\theta = 0°$. At 0° the rearrangement channel contribution along $y \simeq x/2$ is prominent; the node there ($x_2 = 0$) and along $x \simeq 0$ arises from the short-range repulsive nature of the interaction. (At 90° only the incident channel plays a significant role, and $v_4 \equiv 0$.) The absence of significant structure in F means that reasonable approximations to the quartet continuum function can be made if the deuteron is properly included.

The doublet functions are more complex. In Figs. 5 and 6 we plot the F_t and F_s functions, where lower case t and s refer to triplet and singlet, respectively. Because the Pauli principle does not prohibit the close proximity of all three particles for this spin-isospin channel, the short-range repulsive nature of the two-body forces leads to a node in the simplified amplitude F_t from which $\phi_d(x)$ has been factored. The Faddeev amplitudes ψ_t and ψ_s are shown in Figs. 7 and 8; the closed channel feature of ψ_s is very apparent in Fig. 8 where ψ_s approaches zero asymptotically in all directions. It is the sizable difference between ψ_t and ψ_s which accounts for the large mixed-symmetry component of the full Schrödinger wave function in the continuum problem. In Fig. 9 we depict the Faddeev amplitude

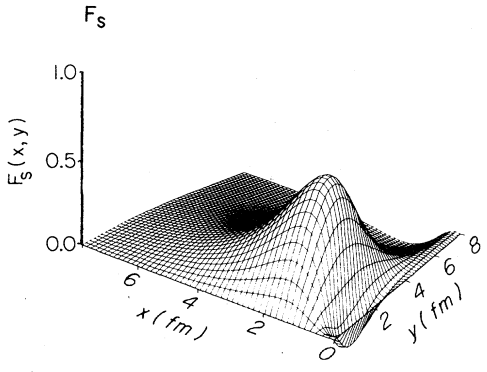

FIG. 6. Faddeev amplitude component F_s for the MT I-III potential model doublet solution.

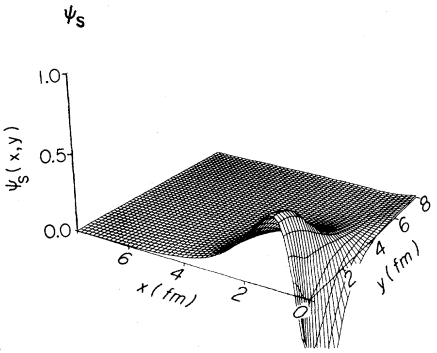

FIG. 8. Faddeev amplitude ψ_s for the MT I-III potential model doublet solution.

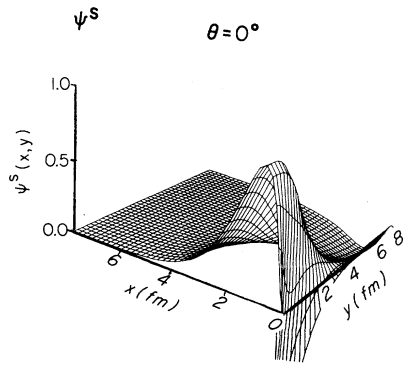

FIG. 9. Faddeev amplitude combination ψ^S for the MT I-III potential model doublet solution.

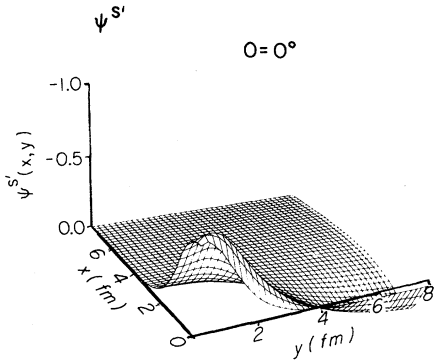

FIG. 11. Faddeev amplitude combination $\psi^{S'}$ for the MT I-III potential model doublet solution.

combination ψ^S used to construct the spatially symmetric wave function component u shown in Fig. 10. This ψ^S is very similar to the corresponding bound state function (see Ref. 4) except for the negative deuteron tail for $y>4$ fm. Short range repulsion leads to the node at small x; the peak results from the strong attraction of the MT I-III potentials for interparticle separations of about 1.0 fm. We remind the reader that, as in the case of the bound state, ψ^S need not be small along $x=0$ for potential models exhibiting strong short range repulsion; it is only the amplitude combination forming $u(x,y)$ which must be small there. The rearrangement channel contribution along $y\simeq x/2$ and the approximate zero along that line are prominent features in Fig. 10. The peaks near $(x,y)=(2.0,0.0)$ fm and (1.0,1.5) fm correspond to the collinear configurations which maximize the number of interparticle separations of approximately 1 fm. The continuum wave function and the ground-state wave function must be orthogonal; thus we find the sign change in u between the origin and the asymptotic region. In Fig. 11 we plot the $\psi^{S'}$ combination of Faddeev amplitudes needed to construct the v_1 and v_2 Schrödinger wave function components shown in Figs. 12 and 13 for $\theta=0°$. The incident and rearrangement channel structures are quite prominent. We reemphasize that v_1 and v_2 are not small compared to u. However, the peaks corresponding to strong attraction for configurations maximizing the interparticle separations of 1 fm are suppressed in v_1 and v_2 compared to those in u. Finally, in Figs. 14 and 15 we plot u and v_1 for $\theta=90°$ to illustrate that the rearrangement channel effects disappear. (A similar simplification of the wave function structure away from $\theta=0°$ occurs for the bound state; see Ref. 4.) For $\theta=90°$, $v_2\equiv 0$.

VII. SUMMARY

We have shown that our computational procedure is sufficiently precise to permit us to generate useful *nd* continuum wave functions for application to the study of such interesting reactions as

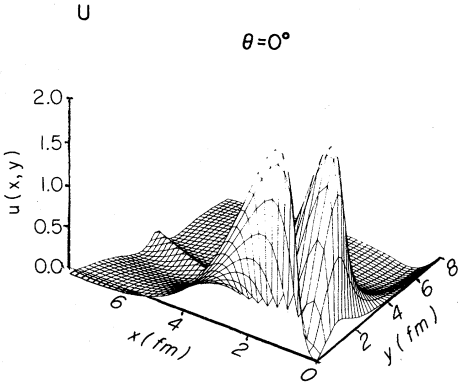

FIG. 10. Doublet Schrödinger wave function component u for the MT I-III potential model at fixed angle $\theta=0°$.

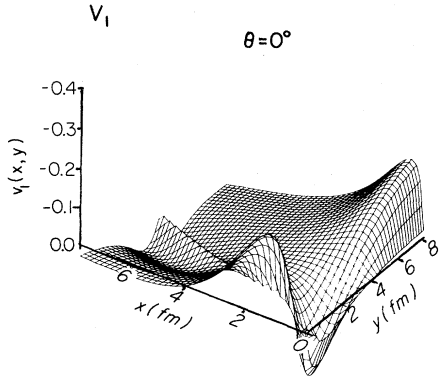

FIG. 12. Doublet Schrödinger wave function component v_1 for the MT I-III potential model at fixed angle $\theta=0°$.

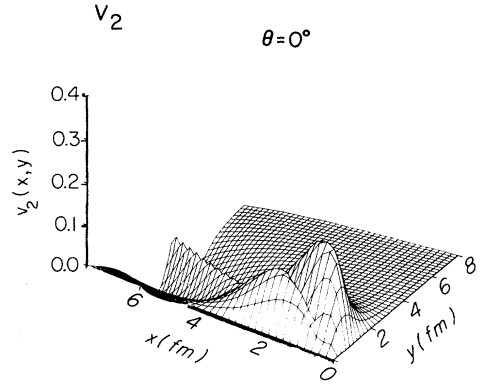

FIG. 13. Doublet Schrödinger wave function component v_2 for the MT I-III potential model at fixed angle $\theta=0°$.

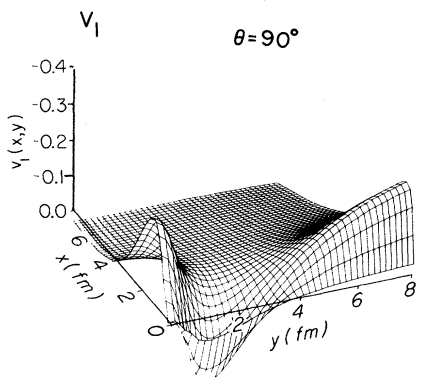

FIG. 15. Doublet Schrödinger wave function component v_1 for the MT I-III potential model at fixed angle $\theta=90°$.

$nd \rightarrow {}^3H\gamma$. Our scattering length results for the Malfliet-Tjon models (with parameters defined in Table I) are in reasonable agreement with previously published results, where they exist. However, comparing our scattering lengths extracted from the configuration space continuum wave functions with Kohn variational estimates provides a much better picture of the accuracy. We find using the most physically realistic of the Malfliet-Tjon models (MT I-III) that the calculated doublet and quartet scattering lengths are $a_2=0.70\pm0.01$ fm and $a_4=6.442\pm0.005$ fm. Thus, the results are in very reasonable agreement with the experimental values[17] of 0.65 ± 0.04 fm and 6.35 ± 0.02 fm considering that there is no tensor force in the model and that the fits to the two-nucleon phase shifts are not that precise.

We have also studied graphically the Faddeev amplitudes and full Schrödinger wave functions for the zero-energy continuum problem. We have identified the important nodes and peaks due to short-range repulsion and strong attraction in the two-body forces as well as the prominent features due to the deuteron structure in the incident and rearrangement channels, the Pauli principle in the quartet state, and the orthogonality (with the ground state) requirement in the doublet state. In particular, we have illustrated the importance of removing the known structure of the deuteron wave function from the asymptotic region, which eases considerably the difficulty of numerically modeling the three-body wave functions there. Our illustration of the complexities of the exact solution should help provide an understanding of why simple approximations to the continuum problem have failed.

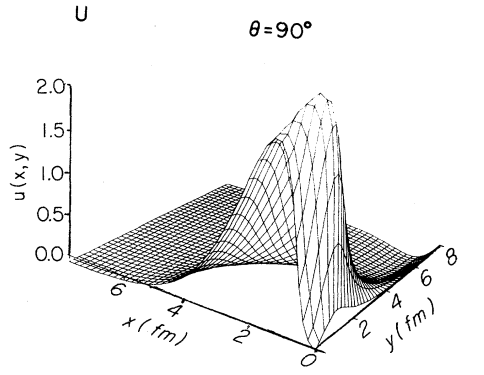

FIG. 14. Doublet Schrödinger wave function component u for the MT I-III potential model at fixed angle $\theta=90°$.

Note added in proof. It has come to our attention that Alt and Bakker[19] have also calculated UPA estimates of a_2 and a_4. Their results are in essential agreement with those of Ref. 8.

ACKNOWLEDGMENTS

The work of J.L.F. and B.F.G. was performed under the auspices of the U. S. Department of Energy; that of G.L.P. was supported in part by the U. S. Department of Energy. G.L.P. also acknowledges several useful discussions with W. L. Klink on the proper treatment of the boundary conditions.

APPENDIX: FERMION EQUATIONS

For the spin-dependent, partial-wave-local potential models of Malfliet and Tjon, the wave function in the doublet case has a singlet and a triplet component. Defining ϕ_s as the reduced amplitude for the singlet component and ϕ_t as the reduced amplitude for the triplet component, one obtains the coupled channel equations:

$$\frac{\partial^2\phi_s}{\partial x_1^{\,2}}+\frac{3}{4}\frac{\partial^2\phi_s}{\partial y_1^{\,2}}-\kappa^2\phi_s-U_s(x_1)\left\{\phi_s+\int_{-1}^{1}d\mu\frac{x_1y_1}{x_2y_2}\left[\tfrac{1}{4}\phi_s(x_2,y_2)-\tfrac{3}{4}\phi_t(x_2,y_2)\right]\right\}=0\,, \tag{A1a}$$

$$\frac{\partial^2\phi_t}{\partial x_1^{\,2}}+\frac{3}{4}\frac{\partial^2\phi_t}{\partial y_1^{\,2}}-\kappa^2\phi_t-U_t(x_1)\left\{\phi_t+\int_{-1}^{1}d\mu\frac{x_1y_1}{x_2y_2}\left[-\tfrac{3}{4}\phi_s(x_2,y_2)+\tfrac{1}{4}\phi_t(x_2,y_2)\right]\right\}=0\,, \tag{A1b}$$

where U_s and U_t are $m/\hbar^2$ times the singlet and triplet components of the two-body interaction. For large values of y_1 we have

$$\begin{aligned}&\phi_s(x_1,y_1)\to 0\,,\\&\phi_t(x_1,y_1)\to(y_1-a)u_d(x_1)\,.\end{aligned} \tag{A2}$$

Following the procedure described in Sec. II for the boson case, we define

$$\begin{aligned}&\phi_s(x_1,y_1)=F_s(x_1,y_1)\,,\\&\phi_t(x_1,y_1)=[y_1-F_t(x_1,y_1)]u_d(x_1)\,.\end{aligned} \tag{A3}$$

Along $\rho=\rho_{\max}$ we have the boundary conditions

$$\begin{aligned}&F_s=0\,,\\&\frac{\partial F_t}{\partial\rho}=0\,.\end{aligned} \tag{A4}$$

In the case of quartet scattering one has only a triplet component, and the single equation describing the continuum wave function is

$$\frac{\partial^2\phi}{\partial x_1^{\,2}}+\frac{3}{4}\frac{\partial^2\phi}{\partial y_1^{\,2}}-\kappa^2\phi-U_t(x_1)\left\{\phi-\tfrac{1}{2}\int_{-1}^{1}d\mu\frac{x_1y_1}{x_2y_2}\phi(x_2,y_2)\right\}=0\,, \tag{A5}$$

where for large values of y_1

$$\phi\to(y_1-a)u_d(x_1)\,. \tag{A6}$$

Thus we write

$$\phi(x_1,y_1)=[y_1-F(x_1,y_1)]u_d(x_1) \tag{A7}$$

and solve for $F(x_1,y_1)$ in the same manner as for the boson case.

In the case of the coupled-channel problem, the relation between the Faddeev amplitude solutions above and the Schrödinger wave function is not as trivial as for the single-channel problem. The amplitudes $\psi_t=\phi_t/(x_1y_1)$ and $\psi_s=\phi_s/(x_1y_1)$ can be combined as

$$\psi^S=\frac{1}{\sqrt{2}}(\psi_s-\psi_t) \tag{A8}$$

and

$$\psi^{S'}=\frac{\sqrt{3}}{2}(\psi_s+\psi_t)\,. \tag{A9}$$

These amplitudes become the basis states for construction of the spatial functions u (completely symmetric) and v_1 and v_2 (mixed symmetric):

$$u=\psi^S(x_1,y_1)+\psi^S(x_2,y_2)+\psi^S(x_3,y_3)\,, \tag{A10}$$

$$v_1=\frac{1}{\sqrt{6}}[\psi^{S'}(x_2,y_2)+\psi^{S'}(x_3,y_3)-2\psi^{S'}(x_1,y_1)]\,, \tag{A11}$$

$$v_2=\frac{1}{\sqrt{2}}[\psi^{S'}(x_3,y_3)-\psi^{S'}(x_2,y_2)]\,. \tag{A12}$$

The full Schrödinger wave function is then

$$\psi=u\phi_0+v_2\phi_1-v_1\phi_2\,, \tag{A13}$$

where ϕ_0 is the fully antisymmetric spin-isospin function and (ϕ_1,ϕ_2) are the spin-isospin functions exhibiting mixed symmetry under the permutation transformation operations. These spin-isospin wave functions should not be confused with the reduced radial wave functions we introduced earlier. (See Schiff[18] for a more complete discussion of the spin and isospin functions of three spin-$\frac{1}{2}$, isospin-$\frac{1}{2}$ particles.)

For the quartet system the Schrödinger wave function is simpler, being constructed from the single Faddeev amplitude ψ:

$$\Psi = -v_3\eta_1 + v_4\eta_2 \ .$$

Where the wave function components v_3 and v_4 are defined by

$$v_3 = \tfrac{1}{2}[\psi(x_2,y_2)+\psi(x_3,y_3)-2\psi(x_1,y_1)] \ ,$$

$$v_4 = \frac{\sqrt{3}}{2}[\psi(x_3,y_3)-\psi(x_2,y_2)] \ .$$

The isospin functions η_1 and η_2 are those of Schiff,[18] and we have suppressed the obvious quartet spin functions.

[1]L. D. Faddeev, Zh. Eksp. Teor. Fiz. 39, 1459 (1960) [Sov. Phys.-JETP 12, 1014 (1961)].

[2]A. N. Mitra, Nucl. Phys. 32, 529 (1962).

[3]G. L. Payne, J. L. Friar, B. F. Gibson, and I. R. Afnan, Phys. Rev. C 22, 823 (1980).

[4]J. L. Friar, B. F. Gibson, and G. L. Payne, Z. Phys. A 301, 309 (1981).

[5]W. Kohn, Phys. Rev. 74, 1763 (1948); S. P. Merkuriev, Nucl. Phys. A283, 395 (1974); J. Nuttal, Phys. Rev. Lett. 19, 473 (1967). For further references, see R. J. Nesbet, *Variational Methods in Electron-Atom Scattering* (Plenum, New York, 1980).

[6]R. A. Malfliet and J. A. Tjon, Nucl. Phys. A127, 161 (1969); our parameters have been determined as described in Ref. 3 in order to reproduce the nucleon-nucleon properties reported by Malfliet and Tjon.

[7]J. A. Tjon, Phys. Rev. D 1, 2109 (1970).

[8]E. Harms and V. Newton, Phys. Rev. C 2, 1214 (1970).

[9]J. J. Benayoun, C. Gignoux, and J. Chauvin, Phys. Rev. C 23, 1854 (1981).

[10]H. P. Noyes, in *Three Body Problem in Nuclear and Particle Physics,* edited by J. S. C. McKee and P. M. Rolph (North-Holland, Amsterdam, 1970), p. 2.

[11]J. J. Benayoun and C. Gignoux, Nucl. Phys. A190, 419 (1972).

[12]A. Laverne and C. Gignoux, Nucl. Phys. A203, 597 (1973).

[13]S. P. Merkuriev, C. Gignoux, and A. Laverne, Ann. Phys. (N.Y.) 99, 30 (1976).

[14]T. Sasakawa and T. Sawada, Sci. Rep. Tohuku Univ., Ser. 8: 1, 119 (1980).

[15]J. L. Friar, B. F. Gibson, and G. L. Payne, Phys. Rev. C 24, 2279 (1981).

[16]R. V. Reid, Ann. Phys. (N.Y.) 50, 411 (1968).

[17]W. Dilg, L. Koester, and W. Nistler, Phys. Lett. 36B, 208 (1971).

[18]L. I. Schiff, Phys. Rev. 133, B802 (1964).

[19]E. O. Alt and B. L. G. Bakker, Z. Phys. A 273, 37 (1975).